Research Article

Modeling and Simulation of a Memristor-Based Sawtooth Signal Generator Using Nonlinear Dopant Drift Memristor Models

Ayvaz Kurtdemir[1] , Reşat Mutlu[1],*

[1]Electronics and Communication Engineering Department, Tekirdağ Namık Kemal University, Çorlu Engineering Faculty, Tekirdağ, TURKEY

Abstract: The new circuit element memristor is under inspection for new types of analog applications. Memristors are already used in some oscillator circuits. Recently, it has been shown that a sawtooth signal generator with a memristor can be made using HP model of TiO_2 memristor and its emulator. HP memristor model is obsolete now. In literature, there are ionic memristor models which uses window functions. In this paper, several well-known nonlinear drift memristor model's usabilities to analyze and simulate such a sawtooth signal generator is examined. Analysis of the sawtooth signal generator is done using five different models. It has been shown solving circuit equations that, for some of the models, the circuit has closed form solutions and some of the solutions are invalid at the memristor boundaries (when the state variable is equal to zero or one). Biolek's window function and a modified Biolek's window function, Zha's window function are found to be the most useful ones to model the memristor throughout its whole operation using simulations made in Matlab/Simulink. Low and high-frequency behavior of the signal generator is also shown.

Keywords: *Memristor, Memristor-based signal generator, Nonlinear dopant drift memristor model, Sawtooth waveform, Window function.*

Nonlineer Sürüklenmeli Memristör Modelleri Kullanılarak Memristör Tabanlı Testere Dişi Sinyal Kaynağının Modellenmesi ve Simülasyonu

Özet: Yeni devre elemanı memristörün yeni tip analog devre uygulamaları inceleme altındadır. Memristörler şu ana kadar bazı osilatör devrelerinde kullanılmıştır. Yakın zamanda, HP memristör modeli ve onun emülatörü kullanılarak bir testeredişi dalga sinyal jeneratörünün yapılabileceği gösterilmiştir. HP memristör modeli artık geçersiz olmuş bir modeldir. Literatürde, pencere fonksiyonu kullanan iyonik memristör modelleri de bulunmaktadır. Bu makalede, bir kaç iyi bilinen nonlineer sürüklenme hızlı memristör modelinin böyle bir testeredişi dalga jeneratörünün analizinde ve benzetiminde kullanılabilirliği analiz edilmiştir. Beş farklı model kullanılarak testeredişi dalga jeneratörünün analizi yapılmıştır. Devre denklemleri çözülerek, bazı modeller için, bu devrenin kapalı fonksiyon şeklinde çözümü olduğu ve bazı çözümlerin memristör sınırlarında (memristör durum değişkeni sıfıra ya da bire eşit olduğunda) geçersiz olduğu gösterilmiştir. Biolek'in pencere fonksiyonu ve bir değiştirilmiş Biolek pencere fonsiyonu olan Zha'nın pencere fonksiyonu Matlab/Simulink programıyla yapılan benzetimler kullanılarak, tüm çalışma bölgesi için en kullanışlı pencere fonksiyonları olarak bulunmuştur. Sinyal jeneratörünün alçak ve yüksek frakans davranışı da gösterilmiştir.

Anahtar kelimeler: Memristör, Memristör modeli, Memristör tabanlı sinyal jeneratörü, Testeredişi dalga şekli, Pencere fonksiyonu.

* Corresponding author.
 E-mail address: rmutlu@nku.edu.tr (R. Mutlu)

1. Introduction

Memristor is a nonlinear circuit element [1]-[4]. Some literature review about memristor and memristive systems can be found in [5]-[10]. The simplest memristor model called linear dopant speed memristor model or HP model is given by an HP research team in 2008 [3]. The drift speed of the doped region is assumed to be constant in this model [3]. There are Nonlinear dopant drift memristor models which try to model memristor more accurately and some of them are given in [11]-[15]. Analog application areas of memristor have become a hot research area [9], [16]-[34]. Chua had suggested a staircase signal generator application even when memristor was just a hypothetical component [1]. A few memristor-based oscillator applications are inspected in [16], [23], [28-34]. It is shown that it is possible to make a memristor-based sawtooth signal generator and it is examined with the HP memristor model and its emulator in [35]. Since HP memristor model is obsolete now, more accurate analysis of the memristor-based sawtooth signal generator must be made.

In this study, nonlinear dopant drift memristor models given in [12]-[15] are used to examine such a generator analytically and with simulations. The equations describing the memristor-based generator are created. Analytical methods are tried to solve them. Symbolic computer algebra systems such as Mathematica, which is available online [36], is also used to quicken the solution process. SimulinkTM toolbox of MatlabTM is used to simulate the generator with a few different nonlinear dopant drift memristor models. The results are interpreted.

The paper is arranged as follows. In the second section, The TiO2 memristor models with nonlinear drift are briefly explained. In the third section, the memristor-based sawtooth signal generator is analyzed using the models and the results are explained. In the fourth section, the simulation results of the sawtooth generator are given. The paper is concluded with the last section.

2. TiO₂ Memristör Models with Nonlinear Dopand Drift

HP memristor model is used to analyze the memristor-based sawtooth generator in [35]. The model is obsolete now. The TiO2 memristor models with window functions which take nonlinear dopant drift into account do exist in the literature [11-15]. These memristor models are briefly explained in this section. They are to be used to examine the memristor-based sawtooth generator in the next section. A memristor model with nonlinear dopant drift can be given as

$$v(t) = R(x)i(t) \qquad (1)$$

$$\frac{dx}{dt} = \frac{\mu R_{on}}{D^2} i(t) f(x) \qquad (2)$$

where $v(t)$ is the memristor voltage, $i(t)$ is the memristor current, $R(x)$ is the memristor or resistance, w is the oxidized lenght of memristor, D is the total length of TiO₂ region, $x = \frac{w}{D}$ is the normalized oxidized lenght of memristor, μ_v is the dopant mobility, R_{ON} is the minimum resistance of the memristor, f(x) is the memristor's window function.

The TiO2 memristor resistance is given as

$$R(x) = R_{OFF} - (R_{OFF} - R_{ON})x \qquad (3)$$

As explained in [3], its resistance ranges from its minimum value R_{ON} to its maximum value R_{OFF}. The window functions of the models are given in Table 1 [11-15]. The window function is a measure of how much a memristor approaches to being an ideal memristor [12]. Evaluation of different memristor models are given in Table 1.

Table 1. Evaluation of Existing Nonlinear Dopant Drift Models

	Strukov	Joglekar	Biolek	Prodromakis	Zha
Resolve boundary conditions	Yes	Yes	Discontinuties	Yes	Yes
Impose non-linear drift over entire D	Yes	Yes	Yes	Yes	Yes
Scalable 0<f(x)<=1	N/A	N/A	Limited	Yes	Yes
Flexibility (control parameter)	N/A	N/A	Yes	Yes	Yes

The window functions in [11,12,14] let dopant speed zero at the boundaries of TiO₂ layer, their memristance/resistance value starts changing when the window function is different than zero, and this means that they have boundary tackle issues. The model in [13] and [15] do not suffer from the issues. Strukov window function is given in [3] and equal to

$$f(x) = x - x^2 \qquad (4)$$

Joglekar window function is given in [12] and equal to

$$f(x) = 1 - (2x - 1)^{2p} \qquad (5)$$

where p is a positive integer and $stp(-i)$ is the unit step function. It is defined as

$$stp(i) = \begin{cases} 1, & i \geq 0 \\ 0, & i < 0 \end{cases} \qquad (6)$$

Prodromakis model is given in [14] and its window function is equal to

$$f(x) = j(1 - (x - 0,5)^2 + 0,75)^p) \qquad (7)$$

A new window function has been proposed by Zha et al in [15]. Zha's window function merges the functions given in [13] and [15]. It allows scaling due to the parameter j and the problem of sticking to boundaries are prevented. It is equal to

$$f(x) = j(1 - (0,25(x - stp(-i))^2 + 0,75)^p) \qquad (8)$$

The window functions are drawn in Figure 1 for several different p values.
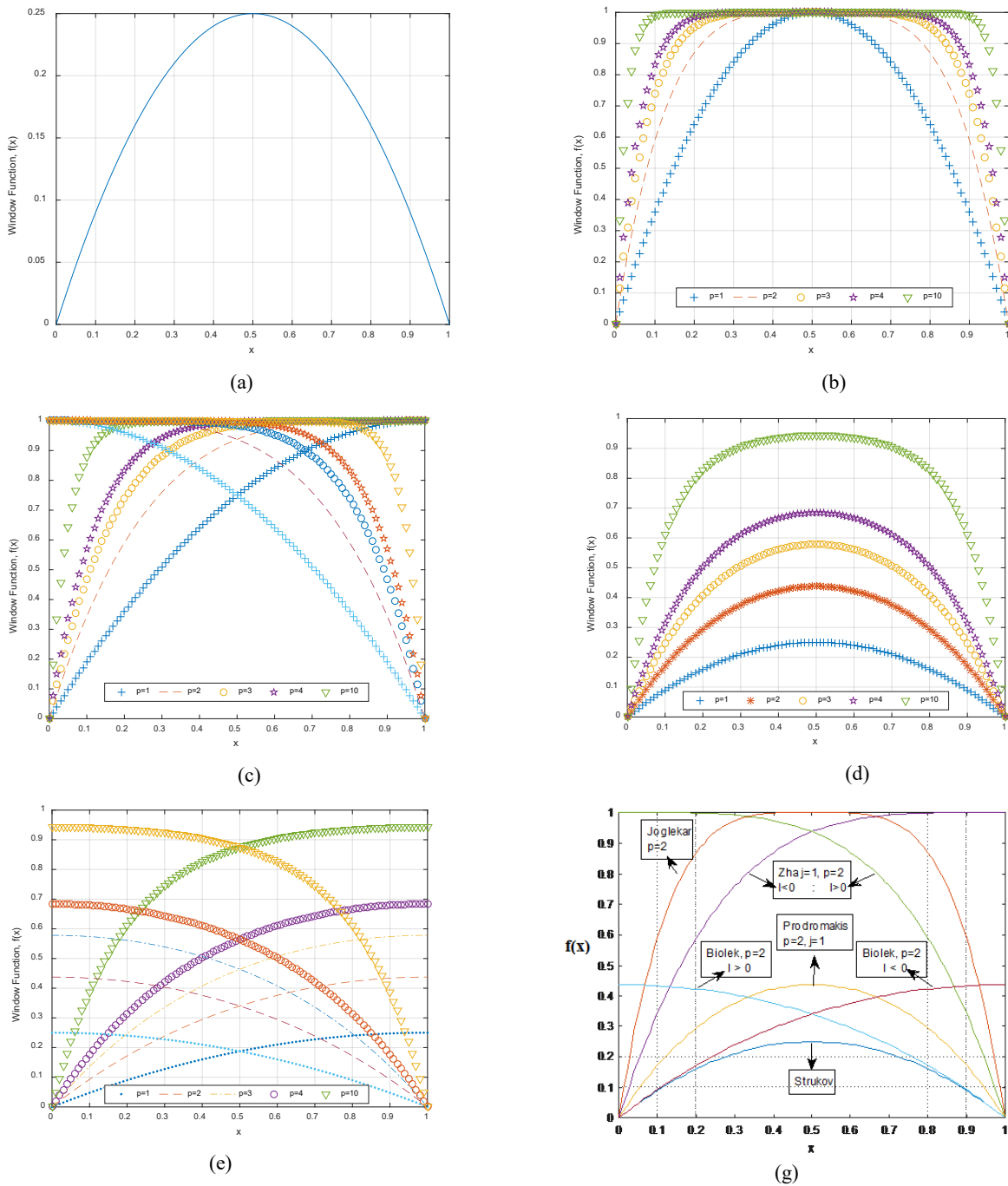
(a)

(b)

(c)

(d)

(e)

(g)

Figure 1. The window functions drawn for 5 different integer p values:
a) Strukov, b) Joglekar, c) Biolek, d) Prodromakis e) Zha

3. Analysis of the Sawtooth Generator with Nonlinear Dopant Drift TiO₂ Memristors Models

The memristor-based sawtooth generator given in [35] is shown in Figure 2. It is made of an opamp-based relaxation oscillator, an opamp voltage follower and the Resistor-Memristor (R-M) inverting amplifier. The opamp voltage follower separates the relaxation oscillator dynamics from the R-M inverting amplifier. The relaxation oscillator is used to obtain a square-wave. The memristor polarity in Figure 3 is chosen as the way that its memristance increases with positive current.
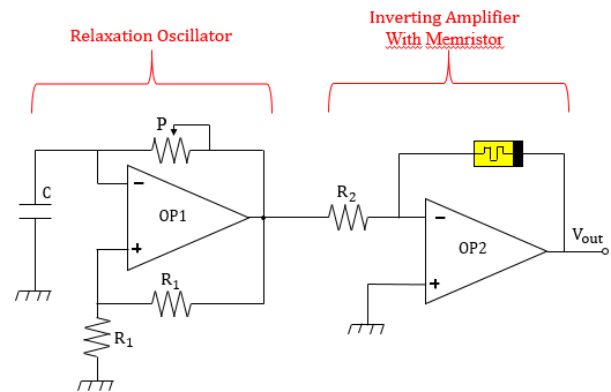

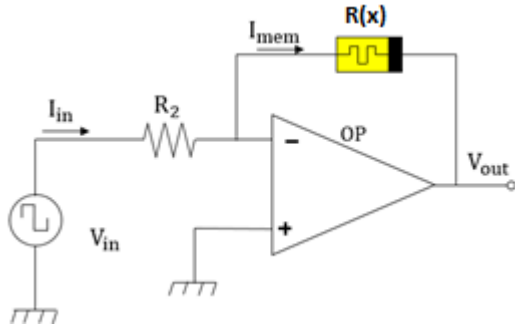**Figure 2.** The sawtooth wave generator with a memristor [35].

Figure 3: The R-M inverting amplifier [35].

The input voltage of the R-M amplifier is the output of the relaxation generator and can be given as,

$$V_{in} = \begin{cases} V_{sat}, & 0 < t < \frac{T}{2} \\ -V_{sat}, & \frac{T}{2} < t < T \end{cases} \quad (9)$$

Where V_{sat} is the saturation voltage of the opamp of the relaxation oscillator and T is the electrical period of the square-wave.

Then, the input current of the R-M amplifier;

$$V_{in} = \frac{V_{in}}{R} = \begin{cases} \frac{V_{sat}}{R}, & 0 < t < \frac{T}{2} \\ -\frac{V_{sat}}{R}, & \frac{T}{2} < t < T \end{cases} \quad (10)$$

where R is the input resistance of the resistor R_2 given in Figures 2 and 3.

The memristor current is also equal to the input current of the R-M amplifier. The output voltage can be written as

$$V_{out} = -\frac{R(x)}{R}V_{in} \quad (11)$$

If the memristor is not in saturation,

$$R(x(t)) = R_{OFF} - (R_{OFF} - R_{ON})x(t) \quad (12)$$

Therefore,

$$V_{out} = -\frac{(R_{OFF}-(R_{OFF}-R_{ON})x(t))}{R}V_{in} \quad (13)$$

Therefore, to obtain the output voltage, the memristor state variable $x(t)$ with respect to time must be known. $x(t)$ is the solution of the following differential function;

$$\frac{dx}{dt} = \frac{\mu_v R_{ON}}{D^2}i(t)f(x) \quad (14)$$

$$\frac{1}{f(x)}\frac{dx}{dt} = \frac{\mu_v R_{ON}}{D^2}i(t) = \frac{\mu_v R_{ON}V_{in}}{RD^2} \quad (15)$$

$$\frac{dx}{f(x)} = \frac{\mu_v R_{ON}V_{in}}{RD^2}dt \quad (16)$$

$$\int \frac{dx}{f(x)} = \int \frac{\mu_v R_{ON}V_{in}}{RD^2}dt = \frac{\mu_v R_{ON}V_{in}}{RD^2}t + C \quad (17)$$

where C is the integration constant.

3.1. Analysis of the Circuit with Strukov Model

Let $k = \frac{\mu_v R_{ON}}{D^2}$ for the sake of simplification. Then, by submitting Strukov window function in Eq. (18), the following equation is

obtained:

$$\int \frac{dx}{x} + \int \frac{dx}{1-x} = \int kIdt \quad (18)$$

By integrating Eq. (18),

$$\ln(x) - \ln(1-x) + C1 = kIt + C2 \quad (19)$$

By rearranging Eq. (19), the state variable is found as

$$x = \frac{e^{kIt+C}}{1+e^{kIt+C}} \quad (20)$$

At t=0, x(0) intitial value can be found as

$$x_0 = (R_{OFF} - R_0)/\Delta R \quad (21)$$

where Ro is the initial memristance value.

Using x(0), the integration constant can be found as

$$C = \ln\left(\frac{x(0)}{1-x(0)}\right) \quad (22)$$

Submitting C into Eq. (23),

$$x = \frac{e^{kIt}x(0)}{1+x(0)(e^{kIt}-1)} \quad (23)$$

Submitting C into Eq. (3), the memristance is found as

$$R(x) = R_{ON}\frac{e^{kIt}x(0)}{1+x(0)(e^{kIt}-1)} + R_{OFF}\left(1 - \frac{e^{kIt}x(0)}{1+x(0)(e^{kIt}-1)}\right) \quad (24)$$

Using Eq. (120, the output voltage is obtained as

$$V_{Out} =$$

$$\begin{cases} \dfrac{R_{ON}\frac{e^{kIt}x(0)}{1+x(0)(e^{kIt}-1)}+R_{OFF}\left(1-\frac{e^{kIt}x(0)}{1+x(0)(e^{kIt}-1)}\right)}{R_2}, & 0 < t < \frac{T}{2} \\[3mm] -\dfrac{R_{ON}\frac{e^{kIt}x(0)}{1+x(0)(e^{kIt}-1)}+R_{OFF}\left(1-\frac{e^{kIt}x(0)}{1+x(0)(e^{kIt}-1)}\right)}{R_2}, & \frac{T}{2} < t < T \end{cases} \quad (25)$$

3.2. Analysis with Joglekar Model

Joglekar et al parameterized the window function using the parameter p. Eq. (17) turns into

$$\int \frac{dx}{1-(2x-1)^{2p}} = \frac{\mu_v R_{ON}V_{in}}{RD^2}t + C \quad (26)$$

The solution of the Eq. (26) are found for a few p values and given in Table 1. Only the solution found for p=1 has an explicit solution. For other p values, the solutions of Eq. (26) is more complex and of closed form. Mathematica is used to obtain the solutions for a few different p values which are given in Table 2. For the solutions obtained p values other than 1, x(t) should be solved using numerical methods. Eq.s (10) and (11) can be used to obtain the output voltage of the circuit.

3.3. Analysis of the Circuit with Biolek Model

Considering current polarity, Biolek's window function can be expressed as

$$\frac{dx}{dt} = \begin{cases} ki[1-(x-1)^{2p}, & i(t) \le 0 \\ ki[1-(x)^{2p}, & i(t) > 0 \end{cases} \quad (27)$$

Using Biolek window function and the parameter p Eq. (17) turns into

$$\int \frac{dx}{1-(x-1)^{2p}} = \frac{\mu_v R_{ON}V_{in}}{RD^2}t + C, i \le 0 \quad (28)$$

$$\int \frac{dx}{1 - (x)^{2p}} = \frac{\mu_v R_{ON} V_{in}}{RD^2} t + C, \qquad i > 0$$

The differential equations are dependent on current polarity and be solved considering the current direction.

The solution of the Eq. (28) are found for a few p values and given in Table 1. Only the solution found for p=1 has an explicit solution. For other p values, the solutions of Eq. (28) are more complex and of closed form. Mathematica is used to obtain the solutions for a few different p values and different

current polarities which are given in Tables 3 and 4 respectively. For the solutions obtained p values other than 1, x(t) should be solved using numerical methods. Eq.s (10) and (11) can be used to obtain the output voltage of the circuit.

3.4. Analysis of the Circuit with Prodromakis Model

Prodromakis Model has two parameters; p and j. It has no current dependence and it also suffers from boundary tackling issues. For Prodromakis window function using the parameter p and j, Eq. (17) turns into

$$\int \frac{dx}{j(1-(x-0,5)^2+0,75)^p)} = \frac{\mu_v R_{ON} V_{in}}{RD^2} t + C \qquad (29)$$

The solution of the Eq. (30) are found for a few p values and given in Table 5. Only the solution found for p=1 has an explicit solution. For other p values, the solutions of Eq. (29) is more complex and of closed form. Mathematica is used to obtain the solutions for a few different p values which are given in Table 3. For the solutions obtained p values other than 1, x(t) should be solved using numerical methods. Eq.s (10) and (11) can be used to obtain the output voltage of the circuit.

3.5. Analysis of the Circuit with Zha Model

Zha's model is obtained by merging Biolek and Prodromakis model. It is scalable and current polarity dependent. Zha Model has two parameters; p and j. Considering current polarity, Zha's window function can be expressed as

$$f(x) = \begin{cases} j(1 - 0,25(x-1)^2 + 0,75)^p), i(t) < 0 \\ j[1 - (0,25x^2 + 0,75)^p, \ i(t) \geq 0 \end{cases} \quad (30)$$

Using Zha's window function and the parameters p and j, Eq. (17) turns into

$$\int \frac{dx}{j(1 - 0,25(x-1)^2 + 0,75)^p)} = \frac{\mu_v R_{ON} V_{in}}{RD^2} t + C, i \leq 0$$

$$(31)$$

$$\int \frac{dx}{j[1 - (0,25x^2 + 0,75)^p} = \frac{\mu_v R_{ON} V_{in}}{RD^2} t + C, i > 0$$

The differential equations are dependent on current polarity and should be solved considering the current direction. The solution of the Eq. (31) are found for a few p values and for j=1 and given in Tables 6 and 7. Only the solution found for p=1 has an explicit solution. For other p values, the solutions of Eq. (31) are more complex and of closed form. Mathematica is used to obtain the solutions for a few different p values and different current polarities which are given in Tables 6 and 7 respectively. For the solutions obtained p values other than 1, x(t) should be solved using numerical methods. Eq.s (10) and (11) can be used to obtain the output voltage of the circuit.

Table 2. Solutions with Joglekar Model.

p	$\int \frac{dx}{f(x)} = \int kIdt$
1	$\int \frac{dx}{4x(1-x)} = \frac{1}{4}(ln(x) - ln(1-x)) + C1 = kIt + C2$
2	$\int \frac{dx}{-16x^4 + 32x^3 - 24x^2 + 8x} =$ $\frac{1}{8}\left(-log(1-x) + log(x) + tan^{-1}\left(\frac{x-1}{x}\right) + tan^{-1}\left(\frac{x}{1-x}\right)\right) + C1 = kIt + C2$
3	$\int \frac{dx}{-64x^6 - 192x^5 - 240x^4 + 160x^3 - 60x^2 + 12x} =$ $\frac{1}{24}\left(-log(4x^2 - 6x + 3) + log(4x^2 - 2x + 1) - 2 log(1-x) + 2 log(x) + 2\sqrt{3}tan^{-1}\left(\frac{1-4x}{\sqrt{3}}\right) -$ $2\sqrt{3}tan^{-1}\left(\frac{3-4x}{\sqrt{3}}\right)\right) + C1 = kIt + C2$
4	$\int \frac{dx}{-256x^8 + 1024x^7 - 1792x^6 + 1792x^5 - 1120x^4 + 448x^3 - 112x^2 + 16x} =$ $\frac{1}{32}(\sqrt{2}log(4x^2 + 2(\sqrt{2} - 2)x - \sqrt{2} + 2) - \sqrt{2} log(4x^2 - 2(\sqrt{2} - 2)x + \sqrt{2} + 2)$ $-2 log(1-x) + 2 log(x) - 4tan^{-1}(1 - 2x) - 2\sqrt{2}tan^{-1}(-2(\sqrt{2}x + \sqrt{2} + 1)$ $+2\sqrt{2}tan^{-1}\left(2(\sqrt{2}x - \sqrt{2} + 1)\right) + C1 = kIt + C2$

5	$\int \frac{dx}{1-(2x-1)^{10}} =$ $\frac{1}{80}(\sqrt{5}-1)\log\left(8x^2 + 2(\sqrt{5}-5)x + 2\left(2 + \frac{1}{2}(1-\sqrt{5}))\right)\right) +$ $(1+\sqrt{5})\log\left(8x^2 + 2(\sqrt{5}-3)x + 2\left(2 + \frac{1}{2}(-1-\sqrt{5}))\right)\right) -$ $(\sqrt{5}-1)\log(8x^2 - 2(\sqrt{5}+3)x + \sqrt{5}+3) -$ $\sqrt{5}+1)\log(8x^2 - 2(\sqrt{5}+5)x + \sqrt{5}+5) - 4\log(1-x) + 4\log(x) -$ $2\sqrt{2(5+\sqrt{5})}\tan^{-1}(\frac{-8x+\sqrt{5}+3}{\sqrt{2(5+\sqrt{5})}}) - 2\sqrt{(10+2\sqrt{5})}\tan^{-1}\left(\frac{-8x+\sqrt{5}+5}{\sqrt{10+2\sqrt{5}}}\right) +$ $2\sqrt{10+2\sqrt{5}} + \tan^{-1}(\frac{8x+\sqrt{5}-5}{\sqrt{10+2\sqrt{5}}}) + 2\sqrt{10+2\sqrt{5}}\tan^{-1}\left(\frac{8x+\sqrt{5}-3}{\sqrt{10-2\sqrt{5}}}\right)) + C1 = kIt + C2$

Table 3. Solutions of the circuit equations for Biolek window function for 5 different values of p and i≤0.

p	$\int \frac{dx}{f(x)} = \int kIdt$
1	$\int \frac{dx}{2x-x^2} = \frac{1}{2}(\ln(x) - \ln(2-x)) + C1 = kIt + C2$
2	$\int \frac{dx}{-x^4+4x^3-6x^2+4x} = \frac{1}{4}\left(-\log(2-x) + \log(x) + \tan^{-1}\left(\frac{x-2}{x}\right) + \tan^{-1}\left(\frac{x}{2-x}\right)\right) + C = kIt + C2$
3	$\int \frac{dx}{-x^6+6x^5-15x^4+20x^3-15x^2+6x} =$ $\frac{1}{12}\left(\log(x^2-3x+3) + \log(x^2-x+1) - 2\log(2-x) + 2\log(x) + 2\sqrt{3}\tan^{-1}\left(\frac{2x-3}{\sqrt{3}}\right) + 2\sqrt{3}\tan^{-1}\left(\frac{2x-1}{\sqrt{3}}\right)\right) + C1 =$ $kIt + C2$
4	$\int \frac{dx}{-x^8+8x^7-28x^6+56x^5-70x^4+56x^3-28x^2+8x} =$ $\frac{1}{16}\left(\sqrt{2}\left(\log(x^2+(\sqrt{2}+2)x - \sqrt{2}+2) - \sqrt{2}\log(x^2-(\sqrt{2}+2)x + \sqrt{2}+2) - 2\log(2-x) + 2\log(x)\right.\right.$ $\left.\left. - 4\tan^{-1}(1-x) - 2\sqrt{2}\tan^{-1}(-\sqrt{2}x + \sqrt{2}+1) + 2\sqrt{2}\tan^{-1}(\sqrt{2}x - \sqrt{2}+1)\right)\right) + C1 = kIt + C2$
5	$\int \frac{dx}{1-(x-1)^{20}} = \frac{1}{80}\left(-(1+\sqrt{5})\log\left(2x^2 + 2\left(\frac{1}{2}(-1-\sqrt{5})-2\right)x + 2\left(2 + \frac{1}{2}(1+\sqrt{5})\right)\right)\right)$ $-(\sqrt{5}-1)\log\left(2x^2 + 2\left(\frac{1}{2}(1-\sqrt{5})-2\right)x + 2\left(2 + \frac{1}{2} + (\sqrt{5}-1)\right)\right)$ $+(\sqrt{5}+1)\log\left(2x^2 + 2\left(\frac{1}{2}(1+\sqrt{5})-2\right)x + 2\left(2 + \frac{1}{2} + (-\sqrt{5}-1)\right)\right)$ $-\sqrt{10+2\sqrt{5}})\log(2x^2 + 2\left(-2 - \sqrt{\frac{1}{2}(5+\sqrt{5})}\right)x + 2\left(2 + \sqrt{\frac{1}{2}(5+\sqrt{5})}\right)$ $+\sqrt{2(5+\sqrt{5})}\log\left(2x^2 + 2\left(\sqrt{\frac{1}{2}(5+\sqrt{5})}-2\right)x + 2\left(2 - \sqrt{\frac{1}{2}(5+\sqrt{5})}\right)\right)$ $-4\log(2-x) + 4\log(x) - 2\sqrt{2(5+\sqrt{5})}\tan^{-1}(\frac{-4x+\sqrt{5}+3}{\sqrt{(10+2\sqrt{5})}})$ $-2\sqrt{(10-2\sqrt{5})}\tan^{-1}\left(\frac{-4x+\sqrt{5}+5}{\sqrt{(10-2\sqrt{5})}}\right) - 2(1+\sqrt{5})\tan^{-1}(\frac{-4x+\sqrt{10-2\sqrt{5}}+4}{1+\sqrt{5}}) + 2(\sqrt{5}-1)\tan^{-1}(\frac{-4x+\sqrt{10+2\sqrt{5}}+4}{1-\sqrt{5}})$

$$-8tan^{-1}(1-x) + 2\sqrt{(10+2\sqrt{5})}tan^{-1}\left(\frac{4x+\sqrt{5}-5}{\sqrt{(10-2\sqrt{5})}}\right) + 2\sqrt{(10-2\sqrt{5})} + tan^{-1}\left(\frac{4x+\sqrt{5}-3}{\sqrt{(10-2\sqrt{5})}}\right) +$$

$$2(\sqrt{5}+1)tan^{-1}\left(\frac{4x+\sqrt{10-2\sqrt{5}}-4}{\sqrt{(1+\sqrt{5})}}\right) + 2(\sqrt{5}-1)tan^{-1}\left(\frac{4x+\sqrt{10-2\sqrt{5}}-4}{\sqrt{(\sqrt{5}-1)}}\right) + C1 = kIt + C2$$

Table 4. Solutions of the circuit equations for Biolek window function for 5 different values of p and I>0.

p	$\int \frac{dx}{f(x)} = \int kIdt$
1	$\int \frac{dx}{1-x^2} = \frac{1}{2}(\ln(x+1) - \ln(1-x)) + C1 = kIt + C2$
2	$\int \frac{dx}{1-x^4} = \frac{1}{4}\left(-\log(1-x) + \log(1+x) + 2tan^{-1}(x)\right) + C1 = kIt + C2$
3	$\int \frac{dx}{1-x^6} = \frac{1}{12}\left(-\log(x^2-x+1) + \log(x^2+x+1) - 2\log(1-x) + 2\log(x+1) + 2\sqrt{3}tan^{-1}\left(\frac{2x-1}{\sqrt{3}}\right) + 2\sqrt{3}tan^{-1}\left(\frac{2x+1}{\sqrt{3}}\right)\right) + C1 = kIt + C2$
4	$\int \frac{dx}{1-x^8} = \frac{1}{16}\left(-\sqrt{2}\log(x^2-\sqrt{2}x+1) + \sqrt{2}\log(x^2+\sqrt{2}x+1) - 2\log(1-x) + 2\log(1+x) + 4tan^{-1}(x) - 2\sqrt{2}tan^{-1}(1-\sqrt{2}x) + 2\sqrt{2}tan^{-1}(\sqrt{2}x+1)\right) + C1 = kIt + C2$
10	$\int \frac{dx}{(1-x^{20})} = \frac{1}{80}\left(-(1+\sqrt{5})\log(2x^2+(-1-\sqrt{5})x+2) - (\sqrt{5}-1)\log(2x^2+(1-\sqrt{5})x+2)\right.$ $-\left(\sqrt{10-2\sqrt{5}}\right)\log\left(2x^2 - \sqrt{(10-2\sqrt{5})}x+2\right) + \left(\sqrt{10-2\sqrt{5}}\right)\log\left(2x^2 + \sqrt{(10-2\sqrt{5})}x+2\right)$ $(\sqrt{5}-1)\log(2x^2+(\sqrt{5}-1)x+2) + (1+\sqrt{5})log(2x^2+(\sqrt{5}+1)x+2)$ $-\left(\sqrt{10+2\sqrt{5}}\right)\log\left(2x^2 - \left(\sqrt{10+2\sqrt{5}}\right)x+2\right) + \left(\sqrt{10+2\sqrt{5}}\right)\log\left(2x^2 + \left(\sqrt{10+2\sqrt{5}}\right)x+2\right)$ $-4\,log(1-x) + 4\,log(x+1) - 2\left(\sqrt{10-2\sqrt{5}}\right)tan^{-1}\left(\frac{4x+\sqrt{5}+1}{\sqrt{(10-2\sqrt{5})}}\right)$ $+2(\sqrt{5}-1)tan^{-1}\left(\frac{\sqrt{10+2\sqrt{5}}-4x}{\sqrt{(1-\sqrt{5})}}\right) + 8tan^{-1}(x) + 2\left(\sqrt{10+2\sqrt{5}}\right) + tan^{-1}\left(\frac{4x-\sqrt{5}+1}{\sqrt{(10+2\sqrt{5})}}\right)$ $+2\left(\sqrt{10+2\sqrt{5}}\right)tan^{-1}\left(\frac{4x+\sqrt{5}-1}{\sqrt{(10+2\sqrt{5})}}\right) + 2\left(\sqrt{10-2\sqrt{5}}\right)tan^{-1}\left(\frac{4x+\sqrt{5}+1}{\sqrt{(10-2\sqrt{5})}}\right)$ $+2(\sqrt{5}+1)tan^{-1}\left(\frac{4x-\sqrt{10-2\sqrt{5}}}{\sqrt{(1+\sqrt{5})}}\right) + 2(\sqrt{5}+1)tan^{-1}\left(\frac{4x-\sqrt{10-2\sqrt{5}}}{\sqrt{(1+\sqrt{5})}}\right)$ $\left. 2(\sqrt{5}-1)tan^{-1}\left(\frac{4x+\sqrt{10+2\sqrt{5}}}{\sqrt{(\sqrt{5}-1)}}\right)\right) + C1 = kIt + C2$

Table 5. Solutions of the circuit equations for Prodromakis window function for 5 different values of p.

$\int \frac{dx}{f(x)} = \int kIdt$

p	
p	$\int \frac{dx}{x-x^2} = lnx - \ln(1-x) + C\,1 = kIt + C2$
1	$\int \frac{dx}{-x^4 + 2x^3 - 3x^2 + 2x} =$ $\frac{1}{2}(\log(x) - \log(1-x)) + 0{,}377964 tan^{-1}(0{,}755929x - 0{,}377964) + C1 = kIt + C2$
2	$\int \frac{dx}{-x^6 + 3x^5 - 6x^4 + 7x^3 - 6x^2 + 3x} =$ $0.333333(-(0274668 + 0298255i)\log(x - (0{,}867893 + 1{,}17701i))$ $-(0274668 - 0298255i)\log(x - (0{,}867893 - 1{,}17701i))$ $+(0274668 - 0298255i)\log(x - (0{,}132107 + 1{,}17701i))$ $+(0274668 + 0298255i)\log(x - (0{,}132107 + 1{,}17701i))$ $-\log(1-x) + \log(x) + C1 = kIt + C2$
3	$\int \frac{dx}{-x^6 + 3x^5 - 6x^4 + 7x^3 - 6x^2 + 3x} =$ $0.333333(-(0274668 + 0298255i)\log(x - (0{,}867893 + 1{,}17701i))$ $-(0274668 - 0298255i)\log(x - (0{,}867893 - 1{,}17701i))$ $+(0274668 - 0298255i)\log(x - (0{,}132107 + 1{,}17701i))$ $+(0274668 + 0298255i)\log(x - (0{,}132107 + 1{,}17701i))$ $-\log(1-x) + \log(x) + C1 = kIt + C2$
4	$\int \frac{dx}{1 - ((x-0{,}5)^2 + 0{,}75)^4} =$ $-0{,}188982 tan^{-1}(0{,}377964 - 0{,}755929x + 0{,}1\log(x^2 - 2x + 2)$ $+0{,}1\log(x^2 + 1) - 0{,}25\log(1-x) + 0{,}25\log(x) - 0{,}1tan^{-1}(1-x)$ $+0{,}1tan^{-1}(x) + C1 = kIt + C2$
10	$-(0{,}0646813 - 0{,}00695034i)\log(x - (1{,}06998 + 0{,}515618i))$ $-(0{,}0646813 + 0{,}00695034i)\log(x - (1{,}06998 - 0{,}515618i))$ $-(0{,}0472654 + 0{,}0122782i)\log(x - (1{,}0506 + 0{,}862932i))$ $-(0{,}0472654 - 0{,}0122782i)\log(x - (1{,}0506 - 0{,}862932i))$ $-(0{,}0325866 + 0{,}0263531i)\log(x - (0{,}92683 + 1{,}11409i))$ $-(0{,}0325866 - 0{,}0263531i)\log(x - (0{,}92683 - 1{,}11409i))$ $-(0{,}0167806 + 0{,}0349125i)\log(x - (0{,}731435 + 1{,}26987i))$ $-(0{,}0167806 - 0{,}0349125i)\log(x - (0{,}731435 - 1{,}26987i))$ $+(0{,}0167806 - 0{,}0349125i)\log(x - (0{,}268565 + 1{,}26987i))$ $+(0{,}0167806 + 0{,}0349125i)\log(x - (0{,}268565 + 1{,}26987i))$ $+(0{,}0325866 - 0{,}0263531i)\log(x - (0{,}07311697 + 1{,}114409))$ $+(0{,}0325866 + 0{,}0263531i)\log(x - (0{,}07311697 - 1{,}114409))$ $+(0{,}0472654 - 0{,}0122782i)\log(x + (0{,}05110612 - 0{,}862932i))$ $+(0{,}0472654 + 0{,}0122782i)\log(x + (0{,}05110612 + 0{,}862932i))$ $+(0{,}0646813 + 0{,}00695034i)\log(x + (0{,}0699814 - 0{,}515618i))$ $+(0{,}0646813 - 0{,}00695034i)\log(x + (0{,}0699814 + 0{,}515618i))$ $-0{,}0755929 tan^{-1}(0{,}377964 - 0{,}755929x) - 0{,}1\log(1-x) + 0{,}1\log(x) + C1 = kIt + C2$

Table 6. Solutions of the circuit equations for Zha's window function for 5 different values of p ve i(t)≤0.

p	$\int dx/fx = \int kIdt$
1	$\int \frac{dx}{1 - (0{,}25(x-1)^2 + 0{,}75)} =$ $= 2\ln(x) - 2\ln(2-x) + C1 = kIt + C2$
2	$\int \frac{dx}{(1 - (0{,}25(x-1)^2 + 0{,}75)^2)} =$ $-\log(2-x) + \log(x) + 0{,}755929 tan^{-1}(0{,}377964(x-1)) + C1 = kIt + C2$
3	$\int \frac{dx}{(1 - (0{,}25(x-1)^2 + 0{,}75)^3)} =$

	$-(0,183112 + 0,193837i)\log(x - (1,73579 + 2,35401i)) - (0,183112 - 0,193837i)\log(x - (1,73579 - 2,35401i)) + (0,183112 - 0,193837i)\log(x - (0,264214 + 2,35401i) + (0,183112 + 0,193837i)\log(x - (0,264214 - 2,35401i) - 0,666667\log(2 - x)\,0,666667\log(x) + C1 = kIt + C2$
4	$\int \frac{dx}{(1-(0,25(x-1)^2+0,75)^4)} =$ $-0,377964 tan^{-1}(0,377964(1 - x)) + 0,2\log(x^2 + 4) - 0,2\log(x^2 - 4x + 8) - 0,5\log(2 - x) + 0,5\log x - 0,2 tan^{-1}(1 - 0,5x) + 0,2 tan^{-1}(0,5x) + C1 = kIt + C2$
10	$\int \frac{dx}{(1-(0,25(x-1)^2+0,75)^{10})} =$ $-(0,129363 - 0,0139007i)\log(x - (2,13996 + 1,03124i))$ $-(0,129363 + 0,0139007i)\log(x - (2,13996 - 1,03124i))$ $-(0,0945307 + 0,0245564i)\log(x - (2,10212 + 1,72586i))$ $-(0,0945307 - 0,0245564i)\log(x - (2,10212 - 1,72586i))$ $-(0,0651733 + 0,0527063i)\log(x - (1,853661 + 2,22818i))$ $-(0,0651733 - 0,0527063i)\log(x - (1,853661 - 2,22818i))$ $-(0,0356613 + 0,069825i)\log(x - (1,462869 + 2,53975i))$ $+(0,0356613 - 0,069825i)\log(x - (1,462869 - 2,53975i))$ $+(0,0356613 - 0,069825i)\log(x - (0,537131 + 2,53975i))$ $+(0,0356613 + 0,069825i)\log(x - (0,537131 - 2,53975i))$ $+(0,0651733 - 0,0527063i)\log(x - (0,146339 + 2,22818i))$ $+(0,0651733 + 0,0527063i)\log(x - (0,146339 - 2,22818i))$ $+(0,0945307 - 0,0245564i)\log(x + (1,10212 - 1,72586i))$ $+(0,0945307 + 0,0245564i)\log(x + (1,10212 + 1,72586i))$ $+(0,129363 + 0,0139007i)\log(x + (1,139963 - 1,03124i))$ $+(0,129363 - 0,0139007i)\log(x + (1,139963 + 1,03124i))$ $-0,2\log(2 - x) + 0,2\log x + 0,151186 tan^{-1}(0,377964 - 0,377964x) + C1 = kIt + C2$

Table 7. Solutions of the circuit equations for Zha's window function for 5 different values of p ve i(t)>0.

p	$\int dx/fx = \int kIdt$
1	$\int \frac{dx}{0,25-0,25x^2}$ $= 2\ln(x + 1) - 2\ln(1 - x) + C1 = kIt + C2$
2	$\int \frac{dx}{1 - (0,25x^2 + 0,75)^2}$ $= -log(1 - x) + log(x + 1) + 0,755929 tan^{-1}(0,377964x) + C1 = kIt + C2$
3	$\int \frac{dx}{1 - (0,25x^2 + 0,75)^3} =$ $-0,183112 log(x^2 - 1,47157x + 6,08276) + 0,183112 log(x^2 + 1,47157x + 6,08276) - 0,666667 log(1 - x) + 0,666667 log(1 + x) + 0,397674 tan^{-1}(0.212403(2x - 1,47157)) + 0,397674 tan^{-1}(0.212403(2x + 1,471157)) + C1 = kIt + C2$
4	$\int \frac{dx}{1 - (0,25x^2 + 0,75)^4} =$ $0,2 tan^{-1}(0,5 - 0,5x) - 0,2\log(x^2 - 2x + 5) + 0,2\log(x^2 + 2x + 5) - 0,5\log(1 - x) + 0,5\log(1 + x) + 0,2\log(0,5x + 0,5) + 0,377964 tan^{-1}(0.377964x)) + C1 = kIt + C2$
10	$\int \frac{dx}{1-(0,25x^2+0,75)^4} =$ $-(0,129363 - 0,0139007i)\log(x - (1,13996 + 1,03124i))$ $-(0,129363 + 0,0139007i)\log(x - (1,13996 - 1,03124i))$ $-(0,0945307 + 0,0245564i)\log(x - (1,10212 + 1,72586i))$

$$-(0{,}0945307 - 0{,}0245564i)\log(x - (1{,}10212 - 1{,}72586i))$$
$$-(0{,}0651733 + 0{,}0527063i)\log(x - (0{,}853661 + 2{,}22818i))$$
$$-(0{,}0651733 - 0{,}0527063i)\log(x - (0{,}853661 - 2{,}22818i))$$
$$-(0{,}0356613 + 0{,}069825i)\log(x - (0{,}462869 + 2{,}53975i))$$
$$-(0{,}0356613 - 0{,}069825i)\log(x - (0{,}462869 - 2{,}53975i))$$
$$+(0{,}0356613 - 0{,}069825i)\log(x + (0{,}462869 - 2{,}53975i))$$
$$+(0{,}0356613 + 0{,}069825i)\log(x + (0{,}462869 + 2{,}53975i))$$
$$+(0{,}0651733 - 0{,}0527063i)\log(x + (0{,}853661 - 2{,}22818i))$$
$$+(0{,}0651733 + 0{,}0527063i)\log(x + (0{,}853661 + 2{,}22818i))$$
$$+(0{,}0945307 - 0{,}0245564i)\log(x + (1{,}10212 - 1{,}72586i))$$
$$+(0{,}0945307 + 0{,}0245564i)\log(x + (1{,}10212 + 1{,}72586i))$$
$$+(0{,}129363 + 0{,}0139007i)\log(x + (1{,}139963 - 1{,}03124i))$$
$$+(0{,}129363 - 0{,}0139007i)\log(x + (1{,}139963 + 1{,}03124i))$$
$$-0{,}2l\og(1 - x) + 0{,}2\log(x + 1) + 0{,}151186tan^{-1}(0{,}377964x) + C1 = kIt + C2$$

4. Simulation Results

As shown in the tables given in the previous section, only for a few cases, the solutions are explicit and they are usually of closed form. The solutions obtained with Strukov, Joglekar and Prodromakis window functions for x=0 and x=1 diverge. Also, the solutions are very complex for p values except for the case for p=1. That's why the memristor-based sawtooth generator circuit must be solved using numerical methods for each window function. Due to space considerations, only Joglekar's, Biolek's and Zha's window functions are used for simulations. The output of the relaxation oscillator is applied to the input of the R-M amplifier. The memristor parameters used in the simulations are shown in Table 8. Simulink toolbox of Matlab is used for simulations. The simulation results of the output voltage of the sawtooth signal generator are shown for the cases of different window functions in the following sections.

Table 8. Memristor parameters used in the simulations.

The memristor minimum resistance	R_{ON}	100 Ohm
The memristor maximum resistance	R_{OFF}	20000 Ohm
The dopant mobility	muon	10^{-14} m^2/V.s
The memristive element length	D	10 nm

4.1. Simulink Results for Joglekar Model

The Simulink block diagram of the Sawtooth Generator for Joglekar window function is shown in Figures 4. Joglekar window function is able to adjust nonlinearity of dopant speed more successfully than Strukov window function due to having the extra parameter p and current polarity dependency. However, it is unable to do scaling considering voltage magnitude and operation frequency. The model is able to simulate the system if the state variable takes values greater than zero and less than 1. As shown in Figure 6 and 7, the state variable x gets stuck at the boundary values at x=0 and x=1 respectively. That's why it

cannot be used to model such a sawtooth generator at x=0 and x=1. Usage of the Joglekar window function to model such a generator must be prevented due to the boundary tackle issues. For x(0)=0.5, there is no boundary tackling issue and a sawtooth waveform at the output is obtained.
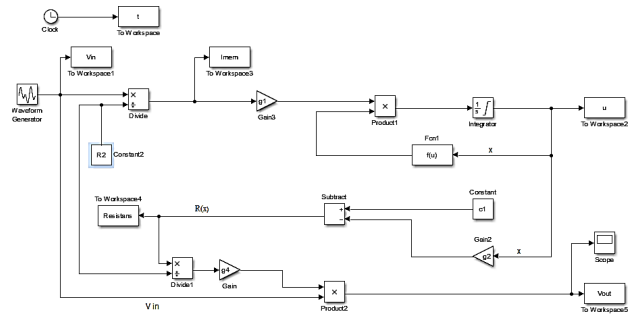

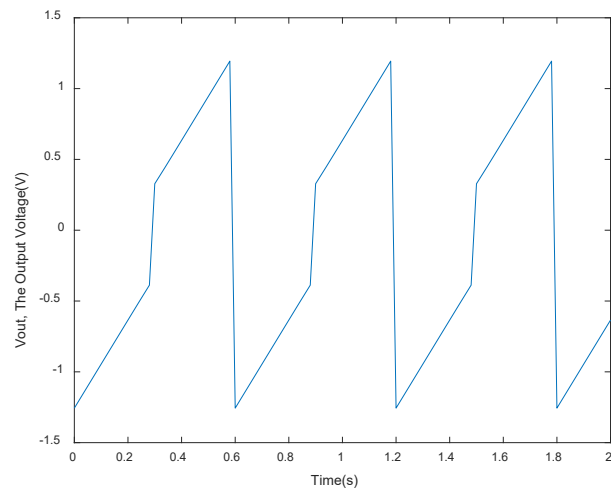**Figure 4.** Simulink block diagram of the Sawtooth Generator for Joglekar's Window Function.

Figure 5. Signal generator output voltage for Joglekar model at 10 Rad/s and $(V_{in})_{pp}$=10 V, R_2=80kΩ, p=5 and x(0)=0.5.
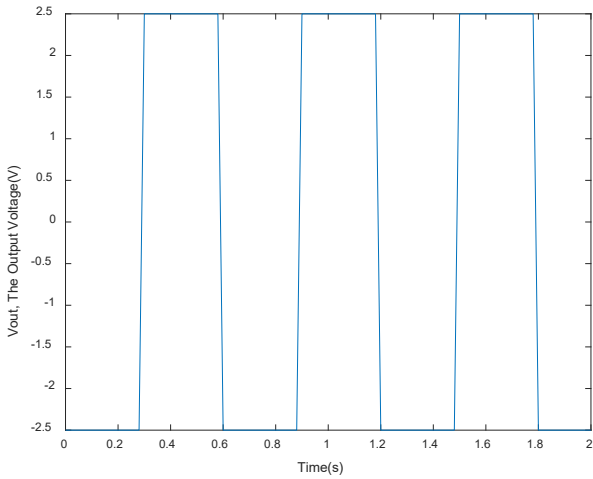
Figure 6. Signal generator output voltage for Joglekar model at 10 Rad/s and $(V_{in})_{pp}=10$, $R_2=80k\Omega$, p=5 and x(0)=0.
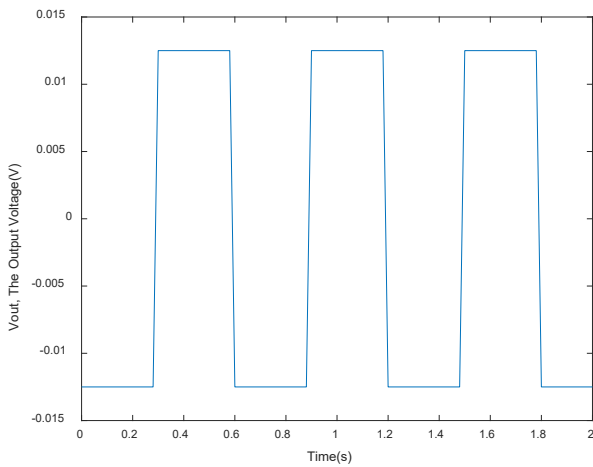

Figure 7. Signal generator output voltage for Joglekar model at 10 Rad/s and $(V_{in})_{pp}=10$, $R_2=80k\Omega$, p=5 and x(0)=1.
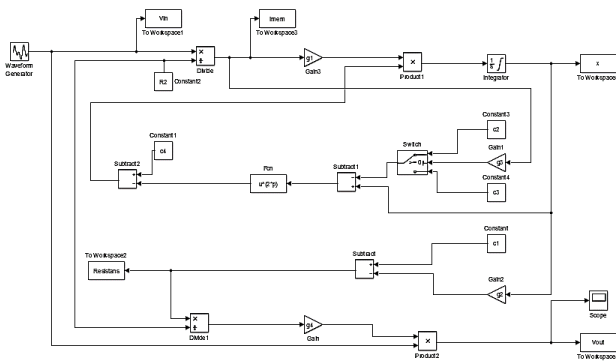

Figure 8. Simulink block diagram of the Sawtooth Generator for Biolek's Window Function.

4.2. Simulink Results for Biolek Model

The Simulink block diagram of the Sawtooth Generator for Biolek Window function is shown in Figures 8. Biolek window function is current-dependent. However, it does not have a scaling parameter as Joglekar. The model is able to simulate the system for the state variable x taking the values between 0 and 1. The output voltage waveforms are very familiar for p=1 and p=2 as shown in Figure 11 and 12 respectively. As shown in Figures 9 through 13, the state variable x does not get stuck at the boundary values at x=0 as and the output voltage is asymmetric due to the current dependency of the Biolek's window function

shown in Figure 11. For 30 rad/s and p=5, the output voltage is shown in Figures 12 and 13. The system output voltage is a sawtooth waveform however it starts resembling a square waveform with increasing frequency.
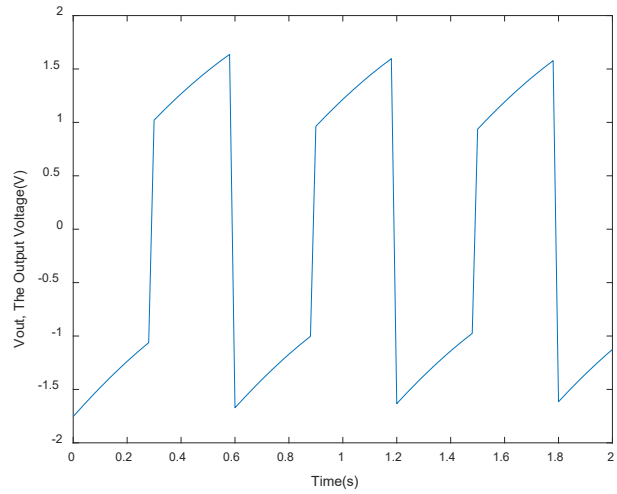
Figure 9. Signal generator output voltage for Biolek model at 10 Rad/s and (Vin)pp=10 V, $R_2=80k\Omega$, p=1 and x(0)=0.3.
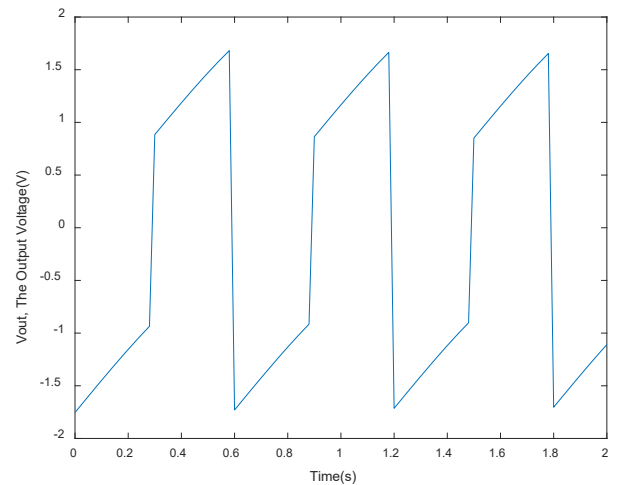
Figure 10. Signal generator output voltage for Biolek model at 10 Rad/s Hz and (Vin)pp=10 V, $R_2=80k\Omega$, p=2 and x(0)=0.3.

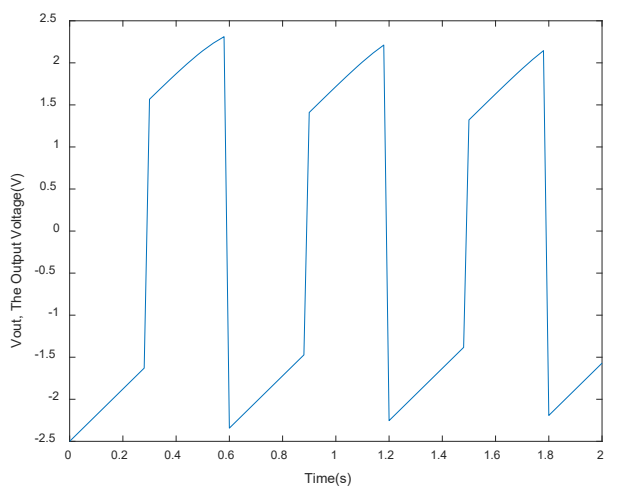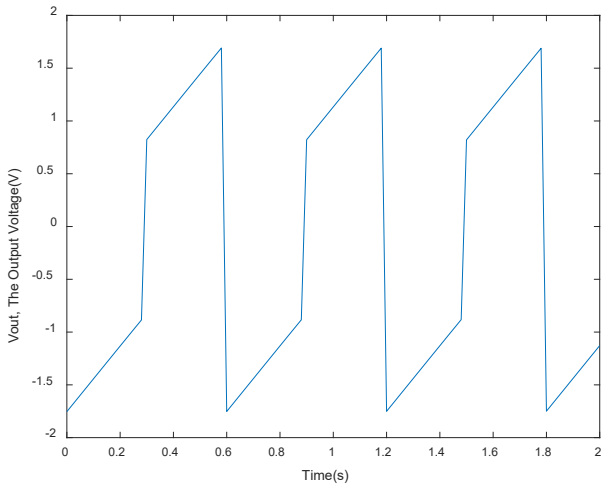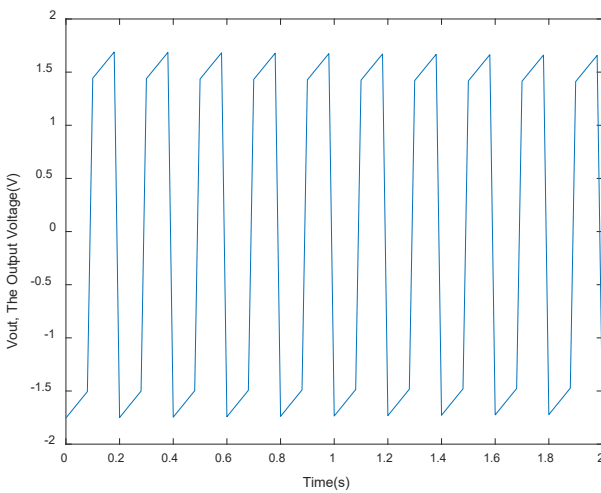**Figure 11.** Signal generator output voltage for Biolek model at 10 Rad/s and (Vin)pp=10 V, $R_2=80k\Omega$, p=5 and x(0)=0.

Figure 12. Signal generator output voltage for Biolek model at 10 Rad/s and (Vin)pp=10 V, R$_2$=80kΩ, p=5 and x(0)=0.3.

Figure 13. Signal Generator Output Voltage for Biolek model at 30 Rad/s and (Vin)pp=10 V, R$_2$=80kΩ, p=5 and x(0)=0.3.

4.3 Simulink Results for Zha Model

The block diagram of the Sawtooth Generator for Zha's Window function is shown in Figures 14. Zha's window function has current dependency as Joglekar's window function and, in addition, it has a scaling parameter. Using different p and j parameter, the waveforms given in Figures 15 through 19 are obtained. An output waveform which looks a sawtooth waveform most can be found in Figure 19. This means that by adjusting memristor parameters, the output voltage waveform of the sawtooth generator can be adjusted. The model is also able to simulate the system without boundary tackling issues. In this case, the state variable x can take all values between 0 and 1 as shown in Figures 19 and 20. The output voltage has a dc offset due to the current dependency of the Zha's window function as shown in Figures 18 through 20. The system output voltage is a sawtooth waveform however it starts resembling a square waveform with increasing frequency. The best-looking sawtooth waveform can be seen in Figure 20. The sawtooth waveform optimization can be done considering the memristor and the other circuit parameters.
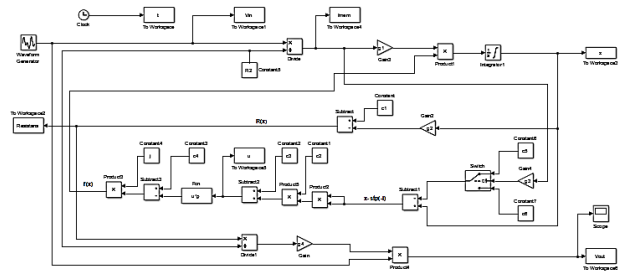

Figure 14. Simulink block diagram of the Sawtooth Generator for Zha's Window Function.
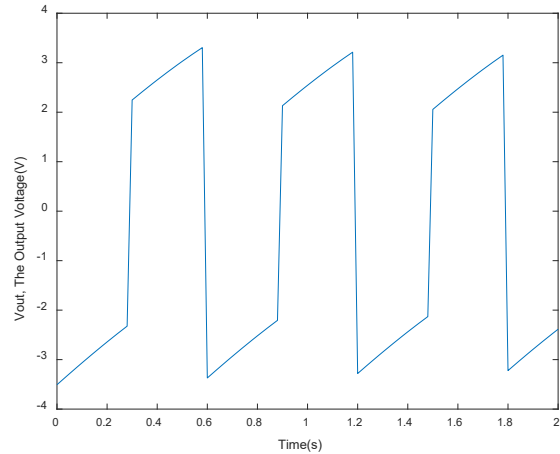

Figure 15. Signal generator output voltage for Zha model at 10 Rad/s and (Vin)pp=10 V, R$_2$=40kΩ, p=5, j=0,5 and x(0)=0,3.

Figure 16. Signal generator output voltage for Zha model at 10 Rad/s and (Vin)pp=10 V, R$_2$=40kΩ, p=5, j=1 and x(0)=0,3.

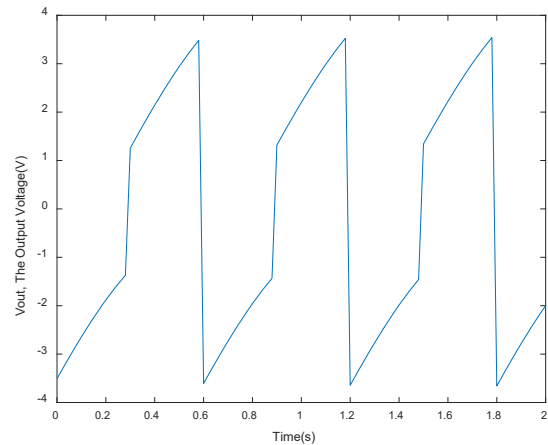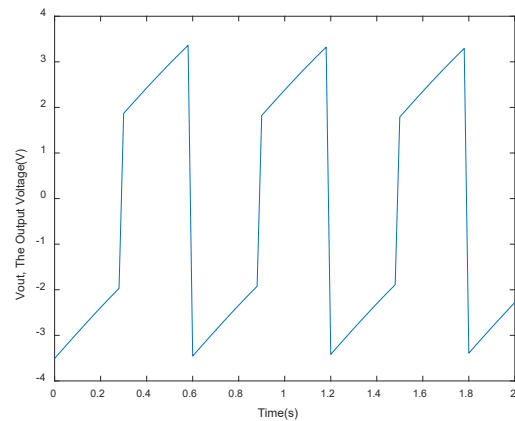**Figure 17.** Signal generator output voltage for Zha model at 10 Rad/s and (Vin)pp=10 V, R$_2$=40kΩ, p=10, j=0,5 ve x(0)=0,3.
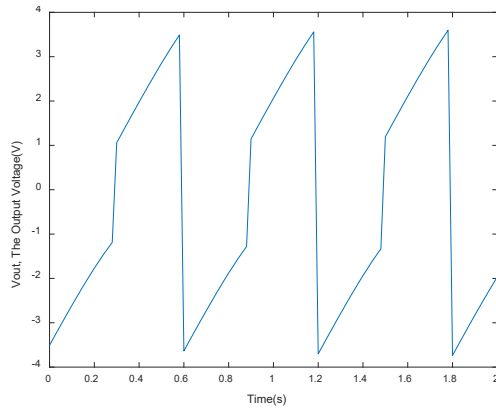
Figure 18. Signal generator output voltage for Zha model at 10 Rad/s and (Vin)pp=10 V, R_2=40kΩ, p=10, j=0,8 and x(0)=0,3.
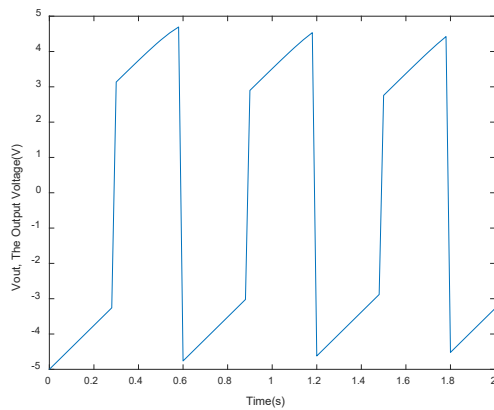

Figure 19. Signal generator output voltage for Zha model at 10 Rad/s and (Vin)pp=10 V, R_2=40kΩ, p=30, j=0.5 ve x(0)=0.
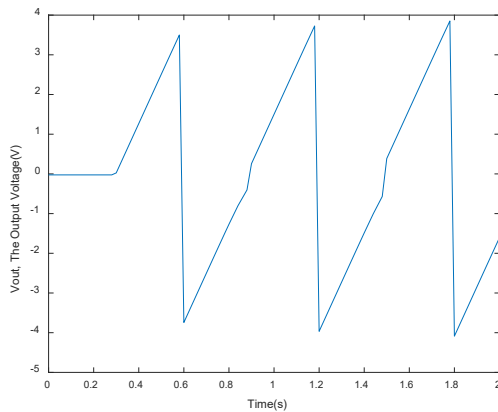

Figure 20. Signal generator output voltage for Zha model at 10 Rad/s and (Vin)pp=10 V, R_2=40kΩ, p=10, j=30 and x(0)=1.
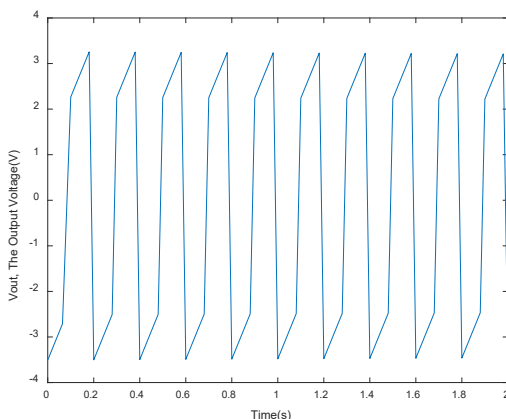

Figure 21. Signal generator output voltage for Zha model at 30

Rad/s and (Vin)pp=10 V, R_2=40kΩ, p=5, j=1 and x(0)=0,3.

5. Conclusion

A sawtooth signal generator given in [35] is examined analytically first using nonlinear dopant drift models. Closed solutions are obtained solving the differential equations describing the memristor-based sawtooth generator. It has become obvious that numerical solutions are needed to simulate the circuit except for a few cases. Simulink is used to simulate the signal generator. The simulated circuit waveforms are obtained and the results are interpreted. As a result of this study, it has been found that Biolek's and Zha's window functions outperform the other nonlinear dopant drift models examined since they do not have the boundary tackling issues. Zha's window function is more flexible due to having a scaling parameter. The memristor-based sawtooth generator may find use in circuits requiring sawtooth waveforms in the future. We suggest that in the design process, such a memristor-based sawtooth generator should be analyzed with future memristor models without the boundary tackling issues.

It is also realized that different models produce different output voltage for the sawtooth generator. If experiments are performed with thin-film memristors, the window function which produces the most similar waveform to the experimental waveform should be chosen for modeling.

In the future, when memristor becomes available in the market, it may be possible to make different types of memristor-based signal generators and mismodeling of a memristor results in mismodeling of such analog application circuits, too. That's why the companies which plan to commercialize memristor should also give models which describes them best to make its exploitation in circuits easier.

References

[1] L. O. Chua, "Memristor - The Missing Circuit Element," IEEE Trans. Circuit Theory, pp. vol. 18, pp. 507-519, 1971.

[2] L. O. Chua ve S. M. Kang, "Memrisive devices and systems," Proc.IEEE, pp. vol. 64, pp. 209-223, 1976.

[3] D. B. Strukov, G. S. Snider, D. R. Stewart, and R. S. Williams," The missing memristor found," Nature (London), Vol. 453, pp. 80-83, 2008.

[4] S. Williams, "How we found the missing memristor," *IEEE Spectrum,* Vol. 45(12), pp. 28–35, 2008.

[5] O. Kavehei, A. Iqbal, Y.S. Kim, K. Eshraghian, S.F. Al-Sarawi and D. Abbott, "The Fourth Element: Characteristics, Modelling, and Electromagnetic Theory of the Memristor," Proceedings of Royal Society A, 2010.

[6] Mazumder, P., Kang, S. M., & Waser, R., "Memristors: devices, models, and applications." Proceedings of the IEEE, 100(6), 1911-1919, 2012.

[7] Kavehei, O., Kim, Y. S., Iqbal, A., Eshraghian, K., Al-Sarawi, S. F., & Abbott, D., "The fourth element: Insights into the memristor," IEEE International Conference on Communications, Circuits and Systems (ICCCAS 2009), pp. 921-927, 2009.

[8] Hu, S. G., Wu, S. Y., Jia, W. W., Yu, Q., Deng, L. J., Fu, Y.

Q., ... & Chen, T. P., "Review of nanostructured resistive switching memristor and its applications," Nanoscience and Nanotechnology Letters, Vol. 6(9), pp. 729-757, 2014.

[9] Pershin, Yu V.; Martinez-Rincon, J.; Di Ventra, M., "Memory circuit elements: from systems to applications," *Journal of Computational and Theoretical Nanoscience*, Vol. 8(3), pp. 441-448, 2011.

[10] Prodromakis, T., "Two centuries of memristors," In Chaos, CNN, Memristors and Beyond: A Festschrift for Leon Chua with DVD-ROM, composed by Eleonora Bilotta, pp. 508-517, 2013.

[11] Yang, J. J., Pickett, M. D., Li, X., Ohlberg, D. A., Stewart, D. R., & Williams, R. S., "Memristive switching mechanism for metal/oxide/metal nanodevices," Nature nanotechnology, 3(7), 429, 2008.

[12] Y. N., Joglekar, and S. J. Wolf. "The elusive memristor: properties of basic electrical circuits." European Journal of Physics 30.4, 661, 2009.

[13] Biolek, Z., Biolek, D., & Biolkova, V., "SPICE model of memristor with nonlinear dopant drift," Radioengineering, Vol. 18(2), pp. 210–214, 2009.

[14] Prodromakis, T., Peh, B. P., Papavassiliou, C., & Toumazou, C., "A versatile memristor model with nonlinear dopant kinetics," IEEE transactions on electron devices, Vol. 58(9), pp. 3099-3105, 2011.

[15] Zha, J., Huang, H., & Liu, Y., "A novel window function for memristor model with application in programming analog circuits," IEEE Transactions on Circuits and Systems II: Express Briefs, Vol. 63(5), 423-427, 2016.

[16] Y. V. Pershin &M. Di Ventra, "Practical approach to programmable analog circuits with memristors," IEEE Transactions Circuits and Systems I: Regular Papers, pp. 57(8), 1857–1864, 2010.

[17] T. Prodromakis, C. Toumazou, "A Review on Memristive Devices and Applications," 17th IEEE International Conference on Electronics, Circuits, and Systems (ICECS), pp. 934 – 937, 2010.

[18] S. Shin, K. Kim, S.M. Kang, "Memristor-based fine resolution programmable resistance and its applications," in ICCCAS 2009 International Conference on Communications, Circuits and Systems, pp. 948–951, 2009.

[19] S. Shin, K. Kim, S.M. Kang, "Memristor applications for programmable analog ICs," IEEE Transactions on Nanotechnology, Vol. 10, pp. 266–274, 2011.

[20] Yi, W., Perner, F., Qureshi, M. S., Abdalla, H., Pickett, M. D., Yang, J. J., ... & Williams, R. S., "Feedback write scheme for memristive switching devices," *Applied Physics A*, *102*(4), pp. 973-982, 2011

[21] T.A. Wey, W.D. Jemison, "Variable gain amplifier circuit using titanium dioxide memristors", IET Circuits, Devices & Systems, Vol. 5, pp. 59–65, 2011.

[22] Berdan, R., T. Prodromakis, and C. Toumazou, "High precision analogue memristor state tuning," Electronics Letters, Vol. 48 (18), pp. 1105-1107, 2012.

[23] D. Yu, H. H. C. Lu, L. A. Fitch & Y. Liang, "A floating memristor emulator based relaxation oscillator," IEEE Transactions on Circuits and Systems – I: Regular Papers, pp. 61(10), 2888–2896, 2014.

[24] A. Ascoli, R. Tetzlaff, F. Corinto, M. Mirchev & M. Gilli, "Memristor-based filtering applications," 14th Latin American Test Workshop (LATW), 2013.

[25] Yener Ş., Mutlu R., Kuntman H. H., "Performance Analysis of a Memristor - Based Biquad Filter Using a Dynamic Model," Journal of Microelectronics, Electronic Components and Materials, vol. 44, pp. 109-118, 2014.

[26] Yener Ş. Ç., Mutlu R., Kuntman H. H., "Small signal analysis of memristor-based low-pass and high-pass filters using the perturbation theory," Optoelectronics and Advanced Materials-Rapid Communications, vol. 12, pp. 55-62, 2018.

[27] Yener Ş., Mutlu R., Kuntman H. H., "A New Memristor-based High-pass Filter/Amplifier: Its Analytical and Dynamical Models," 24th IEEE International Conference Radioelektronika, pp. 1-4, 2014.

[28] Mutlu, R., "Solution of TiO_2 memristor-capacitor series circuit excited by a constant voltage source and its application to calculate operation frequency of a programmable TiO_2 memristor-capacitor relaxation oscillator," Turkish Journal of Electrical Engineering & Computer Sciences, Vol. 23(5), pp. 1219-1229, 2015.

[29] Talukdar A, Radwan AG, Salama KN. "Generalized model for memristor-based Wien-family oscillators," Journal of Microelectronics, Vol. 42, pp. 1032–1038, 2011.

[30] Makoto Itoh and L. O. Chua, "Memristor Oscillators", International Journal of Bifurcation and Chaos, Vol. 18, pp. 3183-3206, 2008.

[31] B. Muthuswamy, "Implementing Memristor Based Chaotic Circuits," International Journal of Bifurcation and Chaos, Vol. 20, p.p. 1335–1350, 2010.

[32] Mosad, A. G., Fouda, M. E., Khatib, M. A., Salama, K. N., & Radwan, A. G., "Improved memristor-based relaxation oscillator," Microelectronics Journal, Vol. 44(9), pp. 814-820, 2013.

[33] Fouda, Mohammed E., Radwan, Ahmed G., "Power dissipation of memristor-based relaxation oscillators", Radioengineering, Vol. 24 (4), pp. 968-973, 2015.

[34] T.A. Wey, S. Benderli, "Amplitude modulator circuit featuring TiO_2 memristor with linear dopant drift," Electronics Letters, Vol 45, p.p. 1103 – 1104, 2009.

[35] Özgüvenç A., Mutlu R., Karakulak E., "Sawtooth signal generator with a memristor," 1st International Conference on Engineering Technology and Applied Sciences (21.04.2016-22.04.2016), 2016.

[36] Online Integral Calculator, "https://www.wolframalpha.com/calculators/integral-calculator/,", July 2019.